


Enhancing of magnetic flux pinning in $\text{YBa}_2\text{Cu}_3\text{O}_{7-x}/\text{CuO}$ granular composites

Cite as: J. Appl. Phys. **118**, 023907 (2015); <https://doi.org/10.1063/1.4926549>

Submitted: 28 April 2015 . Accepted: 27 June 2015 . Published Online: 10 July 2015

A. V. Ushakov, I. V. Karpov, A. A. Lepeshev , and M. I. Petrov



View Online



Export Citation



CrossMark

ARTICLES YOU MAY BE INTERESTED IN

[Low-temperature magnetic behavior of nanostructured ferrite compositions prepared by plasma spraying](#)

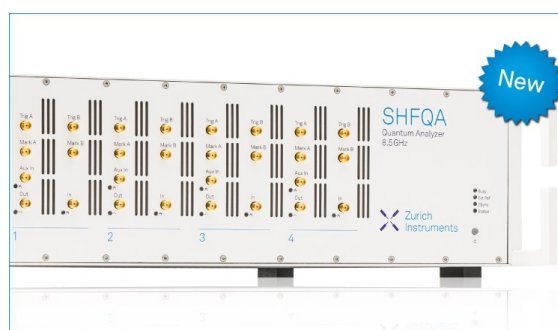
Journal of Applied Physics **122**, 104103 (2017); <https://doi.org/10.1063/1.5001506>

[Magnetization asymmetry of type-II superconductors in high magnetic fields](#)

Journal of Applied Physics **109**, 033904 (2011); <https://doi.org/10.1063/1.3544038>

[High critical currents in heavily doped \(Gd,Y\)Ba₂Cu₃O_x superconductor tapes](#)

Applied Physics Letters **106**, 032601 (2015); <https://doi.org/10.1063/1.4906205>



Your Qubits. Measured.

Meet the next generation of quantum analyzers

- Readout for up to 64 qubits
- Operation at up to 8.5 GHz, mixer-calibration-free
- Signal optimization with minimal latency

Find out more



Enhancing of magnetic flux pinning in $\text{YBa}_2\text{Cu}_3\text{O}_{7-x}/\text{CuO}$ granular composites

A. V. Ushakov,^{1,2} I. V. Karpov,^{1,2} A. A. Lepeshev,^{1,3,a)} and M. I. Petrov³

¹Siberian Federal University, Krasnoyarsk 660041, Russia

²Reshetnev Siberian State Aerospace University, Krasnoyarsk 660014, Russia

³Kirensky Institute of Physics, Russian Academy of Sciences, Siberian Branch, Krasnoyarsk 660036, Russia

(Received 28 April 2015; accepted 27 June 2015; published online 10 July 2015)

This paper shows that the combination of self-assembled structures in the form of “whiskers” and nanoparticles, which appear as a result of the joint sintering powders $\text{YBa}_2\text{Cu}_3\text{O}_{7-x}$ and arc nanopowders CuO, leads to a significant increase in the current density and the appearance of the peak effect in strong magnetic fields range. Very high critical current density appears from a complex vortex pinning, where the defects in the form of “whiskers” provides more energy of pinning, and nanoparticles inhibit the flux creep. Regulation of the morphology of such structures can be achieved by simple change of the concentration of nanodispersed additives. It is shown that the optimal additive is CuO equal to 20 wt. %. © 2015 AIP Publishing LLC.

[<http://dx.doi.org/10.1063/1.4926549>]

I. INTRODUCTION

One of the basic characteristics of superconductors is the critical current density J_c (and, accordingly, the critical current I_c). In cuprate high-temperature superconductors (HTSC), the J_c value at $H = 0$ is very high, but decreases rapidly with increasing H , which limits the use of high-temperature superconductors in electrical power devices and windings of powerful magnets at liquid nitrogen temperature. To increase J_c , the defects, as pinning centers, are deliberately introduced in superconductor, which prevent free movement of magnetic vortices, which leads to energy dissipation. The task is to determine the optimum size and shape of the pinning centers, as well as their number and location in the sample.

After ion irradiation of single crystals of $\text{YBa}_2\text{Cu}_3\text{O}_{7-x}$, a significant increase in J_c is observed; it can reveal that the radiation-induced defects are effective centers of flux pinning.¹ The traditional methods of increasing the critical current density J_c in high-temperature superconductors, such as irradiation by high-energy ions or neutrons, in spite of their certain success, are time consuming and expensive. Obviously, other relatively simple physico-chemical methods of creating artificial pinning centers are required. One of the most promising methods from the technological point of view for creating additional pinning centers and therefore increasing the transport characteristics of HTSC is to introduce nanoscale additives (NSA) of inorganic materials in the superconducting material. It is necessary to choose additives, which are inert to the superconducting matrix. On the one hand, they would not reduce T_c of the source superconductor, and on the other hand, it would play the role of effective pinning centers, when introduced into the superconducting material.

The effective pinning centers, which “fix” vortices, are the inclusions of impurity phases with dimensions equal to

the order of the superconducting coherence length. The features of the pinning in $\text{YBa}_2\text{Cu}_3\text{O}_{7-x}$ nanocomposite films, obtained by the dissolution method and containing randomly oriented non-superconducting “nanodots” BaZrO_3 , Y_2O_3 , BaCeO_3 , and Ba_2YTaO_6 with an average radius of (10–20) nm, are studied in the work.² The record pinning force of more than 20 GN/m³ has been achieved in films with BaZrO_3 content about 10 mol. %.

The authors offered a new model of pinning, whereby deformation of HTSC matrix in the vicinity of nanodots leads to lengthening Cu-O bonds, resulting in the holes decoupling at the neighboring nodes of copper and normal areas of pinning centers are formed.³

Holesinger *et al.* studied the joint effect of the flat and columnar defects obtained by joint chemical deposition of organometallic compounds. These studies showed that the combined effects of random nanoparticles and columnar defects lead to an increase in the critical current density at low and high fields. However, since the microstructural defects are highly dependent on the methods of their growth, there is no assurance that this method allows creating random particles as well as columnar defects. More importantly, it is not easy to control their growth and interaction, maintaining the proper constant composition.⁴

Maiorov *et al.* have developed a method for fabricating $\text{YBa}_2\text{Cu}_3\text{O}_{7-x}$ films using pulsed laser deposition, containing inclusions of BaZrO_3 impurity phases of two types: randomly distributed nanoparticles and columns oriented primarily in one direction (but at a slight angle to each other). The ratio between the concentrations of these defects can be controlled simply by changing the substrate temperature and the film growth rate in the process of laser deposition, which is associated with different kinetics of film formation. The joint analysis of the dependence of J_c from H and microstructure of the films obtained at different conditions showed that J_c in a strong field has its maximum in the case when the number of nanoparticles and “columns” is approximately the

^{a)}Author to whom correspondence should be addressed. Electronic mail: sfu-unesco@mail.ru

same.⁵ The authors of this work explain the obtained results by the suppression of magnetic flux creep due to the expansion of the double kink in the vortex that is attached simultaneously to two “columns.” They suppose that the reason for the lower J_c of single crystals irradiated by heavy ions is the absence of nanoparticles, which are much more effective pinning centers than point radiation defects generated by irradiation at the same time as “columns.” The purpose of this work is to study the influence of the concentration of non-superconducting nanoscale additives of CuO on the superconducting properties of polycrystalline composites CuO-YBa₂Cu₃O_{7-x} at liquid nitrogen temperature.

II. EXPERIMENTAL

Nanodispersed powders (NP) CuO with a characteristic grain size less than 10 nm have been applied to create artificial pinning centers. CuO nanopowder synthesis was carried out in the plasma-chemical reactor.⁶⁻⁹ An arc evaporator was used with the following characteristics: the pulsed arc discharge current of 2.3 kA and the intensity of a longitudinal magnetic field on the surface of the cathode, produced by the focusing coil, of 80 mT. A technological quality copper was chosen as a sputtering cathode. Plasma chemical reactions were implemented by filling with the gas mixture composed of 10% O₂ + 90% Ar in the chamber after the preliminary pumping out to a pressure of 1 MPa. The synthesis was carried out at a pressure of 10 Pa. The cathode was heated up to 700 K before evaporation. The rate of evaporation was measured experimentally by the cathode decrease and was equal to 9 g/min. Nanopowder of copper oxide has been produced during the time of 10 min. Nanopowder of copper oxide had a black color. Weight additive concentrations were 10 and 20 wt. %. A precursor powder YBa₂Cu₃O_{7-x} was obtained by conventional solid phase synthesis. The mixture of YBa₂Cu₃O_{7-x} powders and CuO nanoparticles was stirred in a rotating vessel for 30 h and then was cold pressed in a cylindrical shape with a diameter of 1 mm and a length of 7 mm. Compacting pressure for all samples were similar and equal to 10 MPa. Subsequent high-temperature sintering of tablets of different composition, including a sample without additives, was carried out simultaneously. Sintering is carried out at a temperature of 840 °C for 10 h.

The sample structure was studied by scanning and transmission electron microscopy by electron microscopes JEM-100CX and JEOL JEM-2100.

Magnetization was recorded by differential Hall magnetometry by using two semiconductor Hall sensors switched opposite to the Hall potential outputs. As a result of the apparatus subtraction of the Hall potential of the first Hall sensor from the potential of the second Hall sensor, the resultant signal appeared to be corresponding to the magnetization $M(H)$.

A superconducting solenoid of NbTi was used as a source of the external magnetic field. According to the Bean formula including the demagnetization factor and the dependence of the critical current on the magnetic field, $J_c(H) = 30M(H)/d$, where M is the width of the magnetic hysteresis loop and d is the average size of the crystallite.

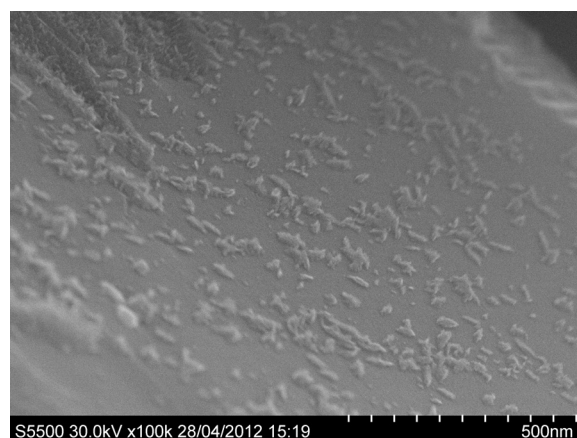
The value $d \sim 6 \mu\text{m}$ was used according to the electron microscopy results. The hysteresis magnetic loops were measured at 70 and 77 K.

The transition temperatures, T_c , were determined from the magnetic transition curves taken after zero-field cooling as the mid-point of these curves with an applied external magnetic field of 2 mT. The transition widths were defined as $\Delta T_c = T_{c0.9} - T_{c0.1}$, where $T_{c0.1}$ and $T_{c0.9}$ were determined as 10% and 90% heights of the transition curve, respectively.

III. RESULTS AND ANALYSIS

Figure 1 shows results of scanning electron microscopy of brittle fracture of the obtained samples at two concentrations of CuO nanosized additives—10 and 20 wt. %.

As it is shown in the figures, after addition of 10 wt. % CuO, the defects are formed as dropshaped inclusions with a maximum drop size of 90–120 nm. After increasing CuO concentration up to 20 wt. %, the inclusions in the form of “whiskers” with the size of 200–300 nm in length as well as droplet defects appear. “Whiskers” have a columnar structure, directed predominantly isotropic. The rounding of the tip is about 10 nm. A statistical analysis of the several hundred defects showed that the average size of the structures in maximum droplet diameter is 65 nm, and the columnar



(a)



(b)

FIG. 1. Changing the microstructure of the composite CuO-YBa₂Cu₃O_{7-x} at the CuO concentration increasing from 10 to 20 wt. %.

structures in basis diameter are 80 nm and 250 nm in length. Fig. 2 shows a typical micrograph of “whiskers” at CuO concentration of 20 wt.%. It was obtained using transmission electron microscopy.

The presented figures show that the “whiskers” have a self-organizing structure consisting of nanocrystallite with an average size of 8 nm. Each “whisker” consists of several smaller “whiskers” with a basis diameter of 20 nm and a length of 80–100 nm. The rounded radius of the tip is 3–5 nm. The phase and elemental analysis showed that the bulk of the “whiskers” consists of non-stoichiometric $\text{CuO}_{0.8}$ with monoclinic lattice with the next parameters: $a = 0.4682$ nm, $b = 0.3421$ nm, and $c = 0.5126$ nm, and practically coincides with the data of the diffraction standards ICDD-JCPDS-38-1420. Certain conclusions can be resulted from the microscopic analysis: (1) The additives of arc CuO nanopowder lead to an increase in non-superconducting CuO inclusions in the structure of the $\text{YBa}_2\text{Cu}_3\text{O}_{7-x}$ granules, which form the pinning centers; (2) Growth of nanostructure defects, their morphology, the ratio between different types of defects, and the direction of growth may be controlled by simply changing the concentration of nanopowder additives.

The critical current density J_c for alloyed and unalloyed YBCO superconductors at 77 K under magnetic field B is shown in Fig. 3 at a x_{CuO} concentration of 10 and 20 wt.%, respectively. The corresponding magnetic transition curves from x_{CuO} concentration are shown in Fig. 4. The sample composites $\text{YBa}_2\text{Cu}_3\text{O}_{7-x}/\text{CuO}$ with 10 wt.% of nano-CuO showed some increase in current density J_c in a magnetic field B in the range from 0 to 1 T, which indicates increased magnetic flux pinning due to the non-superconducting inclusions (Fig. 1). They lead to a distortion of the crystal structure at the interface and influence the distribution of oxygen-deficient areas, as well as to increasing the number of microareas with a low J_c .¹⁰ However, further increase in the magnetic field leads to sufficiently abrupt decrease of a current density down to 0. In this range of magnetic field, the

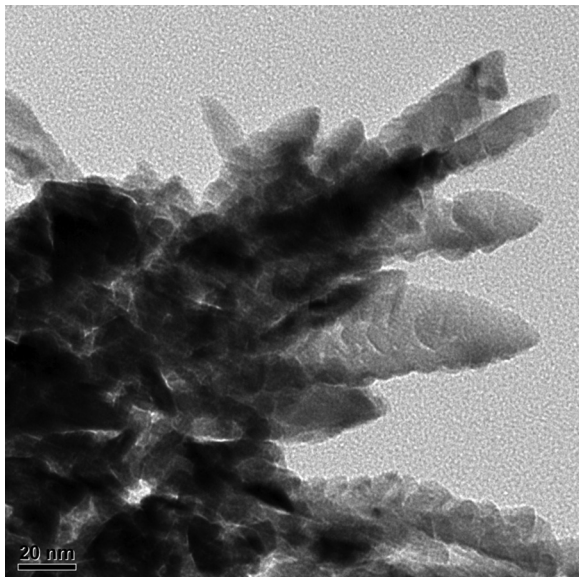


FIG. 2. TEM micrograph of columnar defects formed during the production of the composite $\text{YBa}_2\text{Cu}_3\text{O}_{7-x} + 20$ wt.% CuO.

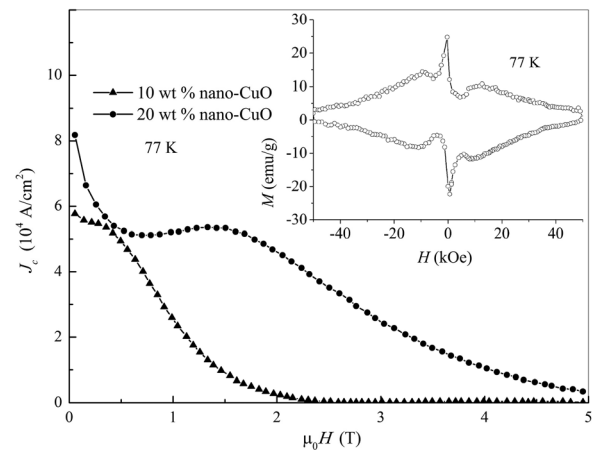


FIG. 3. The dependence of critical current density J_c of magnetic field B for $\text{YBa}_2\text{Cu}_3\text{O}_{7-x}/\text{CuO}$ composites with nano-CuO concentration of 10 and 20 wt.% at 77 K. Inset: M - H loop for $\text{YBa}_2\text{Cu}_3\text{O}_{7-x}/\text{CuO}$ composites with nano-CuO concentration of 20 wt.% at 77 K.

dissipation occurs according to the Arrhenius law $R \approx \exp(-U(H)/T)$,¹¹ which is characteristic for the magnetic flux creep model with temperature-independent energy pinning $U(H)$.^{12–16} As can be seen from Fig. 4, the introduction of 10 wt.% CuO nanopowder leads to a decrease in the critical temperature T_c and the increase in the transition zone width, which confirms the above assumption. Fig. 5 shows the dependence of the critical current density J_c on the magnetic field B for composites $\text{YBa}_2\text{Cu}_3\text{O}_{7-x}/\text{CuO}$ with 10 and 20 wt.% of CuO at 70 K.

The critical current density J_c of the samples is significantly increased under magnetic field B in the range from 0 to 1 T, but the overall behavior of the curve remains typical, as it is for 77 K. The composite samples $\text{YBa}_2\text{Cu}_3\text{O}_{7-x}/\text{CuO}$ with 20 wt.% of nano-CuO show a substantial increase in the critical current density J_c in the whole range of the applied magnetic field B (Fig. 3). In addition, the samples show a clear peak effect in the range of magnetic fields B from 1 to 2 T. Comparing the graphs (Fig. 3) for composites $\text{YBa}_2\text{Cu}_3\text{O}_{7-x}/\text{CuO}$ with 10 and 20 wt.% of CuO and their micrographs (Fig. 1), it becomes obvious that in the range of magnetic field B from 0 to 1 T, the increase in magnetic flux pinning occurs due to drop-shaped non-superconducting

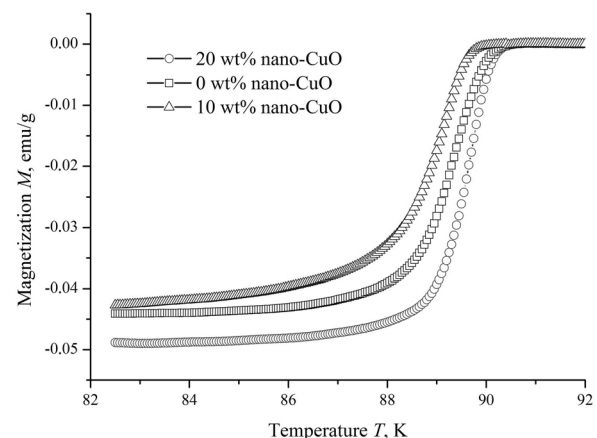


FIG. 4. Magnetic transition curves from x_{CuO} concentration taken after zero-field cooling with an applied external magnetic field of 2 mT.

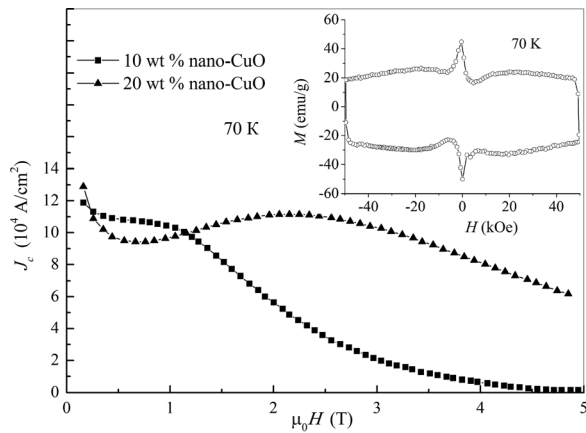


FIG. 5. The dependence of the critical current density J_c of magnetic field B for $\text{YBa}_2\text{Cu}_3\text{O}_{7-x}/\text{CuO}$ composites with CuO concentration of 10 and 20 wt. % at 70 K. Inset: M - H loop for $\text{YBa}_2\text{Cu}_3\text{O}_{7-x}/\text{CuO}$ composites with nano-CuO concentration of 20 wt. % at 70 K.

CuO inclusions. Whereas, in the range of magnetic fields B from 1 to 5 T for composites $\text{YBa}_2\text{Cu}_3\text{O}_{7-x}/\text{CuO}$ with 20 wt. % of CuO increase in the critical current density J_c , and especially, the peak effect is probably the result of non-superconducting inclusions of CuO as “whiskers.” Such composites are characterized by a complex interaction of two types of defects—drops and “whiskers.”

The peak effect represents the broadening of the magnetization hysteresis loop M in the zone of intermediate fields (above the penetration field H_p) and the appearance of the second maximum in the graph of relation of the critical current as function of the field and temperature.^{17,18} In Refs. 18 and 19, it was shown that the defects associated with the peak effect should represent topologically closed system of zones with weak superconductivity, changing to a normal state in the fields of the second maximum in the graph of relation $M(H)$. It was also shown that the system of weak coupling occurs most likely in the areas with lack of oxygen.¹⁸ In Ref. 20, it was shown that the peak effect is also clearly seen in the area of $T > 60$ K. Kwok *et al.* showed that the appearance of the peak effect is associated with pinning intensification due to the softening of the vortex lattice before its melting (melting-transition).^{21,22} It can be assumed that only the extended defects are responsible for the peak effect, while the YBCO superconductors have several types of pinning defects. In this case, the role of such defects is played by non-superconducting inclusion of CuO in the form of “whiskers,” which leads to significant distortion of the lattice vortex. It is shown that a magnetic field penetrates the superconductor only along the direction of the “whiskers.” However, Figure 1 shows that the distance between the whiskers is sufficiently large (about $1 \mu\text{m}$). This allows to conclude that the efficiency of the magnetization due to the pinning depends on the relationship between defects in the form of droplets and defects in the form of “whiskers.” Fig. 5 is a quite clear confirmation of this concept.

In addition to a substantial increase in the critical current density J_c for composite $\text{YBa}_2\text{Cu}_3\text{O}_{7-x}/\text{CuO}$ with 20 wt. % of CuO peak effect shows the temperature dependence. For 77 and 70 K, peak value of B_p is, respectively, 1.5 and 2.5 T. The

defects with the shape of “whiskers” influence on the critical temperature T_c and the width of the transition zone ΔT_c , as it is confirmed by Fig. 4. For the composite $\text{YBa}_2\text{Cu}_3\text{O}_{7-x}/\text{CuO}$ with 20 wt. % of CuO, these values are, respectively, 91 and 0.5 K. The models of increasing the transition temperature in superconductor (T_c), caused by defects in the crystal, determining the long-range deformation, are presented.²³ It is shown that the effect of deformation, introduced by defects, that changes T_c , is noticeably increased in the HTSC due to the increase of the coherence length and the strong anisotropic dependence of the bulk values of T_c on pressure.²⁴ Deformation associated with defects in the form of “whiskers” may be strong enough, causing local plastic deformation or structural transformations around arrays of dislocations. The increase in T_c can be estimated for edge dislocations,^{25,26} the low-angle grain boundaries and metastable linear dislocation arrays based on anisotropic strain dependence of T_c in the ab plane and the proximity effect, which determines the superconducting state on the intercrystallite borders. In addition, changes in composites $\text{YBa}_2\text{Cu}_3\text{O}_{7-x}/\text{CuO}$ with 20 wt. % of CuO, caused by fields of deformation from defects and the effect of changing T_c influence the magnetic flux pinning and magnetic granularity.

The most effective pinning can occur as a result of an appropriate combination of defects.²⁷ The aim of the work should be not to increase the number of defects but to use them in the most effective way, for example, the method of combining different types of defects. In particular, methods for constraining the negative effects of thermal fluctuations are almost unstudied. While the task of obtaining defects by introducing various kinds of nanoparticles is currently completely solvable, the problems associated with growing columnar defects such as “whiskers,” are currently not investigated. Practically, it is very important that the granular superconductors are obtained by the optimal technology, and the value J_c is practically independent from the orientation of the magnetic field.

IV. CONCLUSION

Therefore, the introduction of up to 20 wt. % of non-superconducting nanoscale powders CuO, obtained in the plasma low pressure arc discharge in the polycrystalline HTSC $\text{YBa}_2\text{Cu}_3\text{O}_{7-x}$, can allow producing a new type of composites with nanoscale defects in the form of drops and “whisker.” The study of the superconducting properties of the composites showed a significant increase in the critical current density and the peak effect in strong magnetic fields. The main contribution to the pinning force is made by defects in the form of “whiskers,” while auxiliary pinning on the drops prevents creeping. Defects in the form of “whiskers” are responsible for the increase of the critical temperature T_c and the decrease of width of the transition zone ΔT_c .

ACKNOWLEDGMENTS

This work was supported in part by the Ministry of Education and Science of the Russian Federation (Project No. 11.370.2014/K).

- ¹M. Haruta, T. Fujiiyoshi, T. Sueyoshi, K. Miyahara, T. Ikegami, K. Ebihara, R. Miyagawa, N. Ishikawa, S. Awaji, and K. Watanabe, *Physica C* **412–414**, 511 (2004).
- ²J. L. MacManus-Driscoll, S. R. Foltyn, Q. X. Jia, H. Wang, A. Serquis, L. Civale, B. Maiorov, M. E. Hawley, M. P. Maley, and D. E. Peterson, *Nat. Mater.* **3**, 439 (2004).
- ³A. Llordes, A. Palau, J. Gazquez, M. Coll, R. Vlad, A. Pomar, J. Arbiol, R. Guzman, S. Ye, V. Rouco, F. Sandiumenge, S. Ricart, T. Puig, M. Varela, D. Chateigner, J. Vanacken, J. Gutierrez, V. Moshchalkov, G. Deutscher, C. Magen, and X. Obradors, *Nat. Mater.* **11**, 329 (2012).
- ⁴T. G. Holesinger, L. Civale, B. Maiorov, D. M. Feldmann, J. Y. Coulter, D. J. Miller, V. A. Maroni, Z. Chen, D. C. Larbalestier, R. Feenstra, X. Li, Y. Huang, T. Kodenkandath, W. Zhang, M. W. Rupich, and A. P. Malozemoff, *Adv. Mater. Prog. Rep.* **20**, 391 (2008).
- ⁵B. Maiorov, S. A. Baily, H. Zhou, O. Ugurlu, J. A. Kennison, P. C. Dowden, T. G. Holesinger, S. R. Foltyn, and L. Civale, *Nat. Mater.* **8**, 398 (2009).
- ⁶A. V. Uschakov, I. V. Karpov, A. A. Lepshev, and L. Yu. Fedorov, *Remont, Vosstanovlenie, Modernizatsiya* **9**, 41 (2012) (in Russian).
- ⁷A. V. Uschakov, I. V. Karpov, A. A. Lepshev, and L. Yu. Fedorov, *Technologiya Metallov*, **2**, 35 (2013) (in Russian).
- ⁸I. V. Karpov, A. V. Uschakov, L. Yu. Fedorov, and A. A. Lepshev, *Tech. Phys.* **59**, 559 (2014).
- ⁹A. V. Uschakov, I. V. Karpov, A. A. Lepshev, L. Yu. Fedorov, and A. A. Shajkhudinov, *Materialovedenie* **7**, 29 (2013) (in Russian).
- ¹⁰A. V. Uschakov, I. V. Karpov, A. A. Lepshev, M. I. Petrov, and L. Yu. Fedorov, *JETP Lett.* **99**, 99 (2014).
- ¹¹T. T. M. Palstra, B. Batlogg, R. B. van Dover, L. F. Schneemeyer, and J. V. Waszczak, *Appl. Phys. Lett.* **54**, 763 (1989).
- ¹²P. W. Anderson, *Phys. Rev. Lett.* **9**, 309 (1962).
- ¹³D. A. Balaev, S. I. Popkov, K. A. Shajkhudinov, and M. I. Petrov, *Phys. Solid State* **48**, 826 (2006).
- ¹⁴D. M. Gokhfeld, D. A. Balaev, M. I. Petrov, S. I. Popkov, K. A. Shajkhudinov, and V. V. Val'kov, *J. Appl. Phys.* **109**, 033904 (2011).
- ¹⁵K. A. Shajkhudinov, S. V. Semenov, S. I. Popkov, D. A. Balaev, A. A. Bykov, A. A. Dobrovskiy, M. I. Petrov, and N. V. Volkov, *J. Appl. Phys.* **109**, 083711 (2011).
- ¹⁶D. A. Balaev, S. I. Popkov, E. I. Sabitova, S. V. Semenov, K. A. Shajkhudinov, A. V. Shabanov, and M. I. Petrov, *J. Appl. Phys.* **110**, 093918 (2011).
- ¹⁷R. B. van Dover, E. M. Gregory, L. F. Schneemeyer, J. W. Mitchell, K. V. Rao, R. Puzniak, and J. W. Waszczak, *Nature* **342**, 55 (1989).
- ¹⁸M. Daeumling, J. M. Seuntjens, and D. C. Larbalestier, *Nature* **346**, 332 (1990).
- ¹⁹M. S. Osofsky, J. L. Cohn, E. F. Skelton, M. M. Miller, R. J. Soulen, S. A. Wolf, and T. A. Vanderah, *Phys. Rev. B* **45**, 4916 (1992).
- ²⁰L. Krusin-Elbaum, L. Civale, V. M. Vinokur, and F. Holtzberg, *Phys. Rev. Lett.* **69**, 2280 (1992).
- ²¹W. K. Kwok, J. A. Fendrich, S. Fleshler, U. Welp, and W. Crabtree, "Critical currents in superconductors," in *Proceedings of the 7th International Workshop*, edited by H. W. Weber (Alpbach, Austria, 1994), p. 15.
- ²²W. K. Kwok, J. A. Fendrich, C. J. van der Beek, and W. Crabtree, *Phys. Rev. Lett.* **73**, 2614 (1994).
- ²³A. Gurevich and E. A. Pashitskii, *Phys. Rev. B* **56**, 6213 (1997).
- ²⁴R. J. Wijngaarden and R. Griessen, *Studies on High Temperature Superconductors*, edited by A. V. Narlikar (NovaScience, New York, 1989), Vol. 2, p. 29.
- ²⁵N. Browning, M. F. Chisholm, S. J. Pennycook, D. P. Norton, and D. H. Lowndes, *Phys. C* **212**, 185 (1993).
- ²⁶S. E. Babcock and J. L. Vargas, *Annu. Rev. Mater. Sci.* **25**, 193 (1995).
- ²⁷J. Sosnowski, *Mod. Phys. Lett. B* **28**, 1450132 (2014).